

## Linköping University Post Print

# Impact of cysts during radio frequency (RF) lesioning in deep brain structures: a simulation and in-vitro study

Johannes D. Johansson, Dan Loyd, Karin Wårdell and Joakim Wren

N.B.: When citing this work, cite the original article.

### Original Publication:

Johannes D. Johansson, Dan Loyd, Karin Wårdell and Joakim Wren, Impact of cysts during radio frequency (RF) lesioning in deep brain structures: a simulation and in-vitro study, 2006, Journal of Neural Engineering, (4), 2, 87-95.

<http://dx.doi.org/10.1088/1741-2560/4/2/009>

Copyright: Institute of Physics Publishing

<http://www.iop.org/>

Postprint available at: Linköping University Electronic Press

<http://urn.kb.se/resolve?urn=urn:nbn:se:liu:diva-13997>

# **Impact of cysts during radio frequency (RF) lesioning in deep brain structures – a simulation and in-vitro study**

**Johannes D Johansson<sup>1</sup>, Dan Loyd<sup>2</sup>, Karin Wårdell<sup>1</sup> and Joakim Wren<sup>2</sup>**

<sup>1</sup>Department of Biomedical and Engineering, Linköping University, Linköping, Sweden

<sup>2</sup>Department of Mechanical Engineering, Linköping University, Linköping, Sweden

## ***Corresponding author***

Johannes D Johansson  
Department of Biomedical Engineering  
Linköping University  
581 85 Linköping, Sweden  
Phone: +46-13 222464  
Fax: +46-13 101902  
E-mail: johjo@imt.liu.se

## ***Keywords***

*RF-ablation, Virchow-Robin spaces, natural convection, FEM analysis, Neurosurgery*

## ***Abstract***

Radio frequency lesioning of nuclei in the thalamus or the basal ganglia can be used in order to reduce symptoms caused by e.g. movement disorders such as Parkinson's disease. Enlarged cavities containing cerebrospinal fluid (CSF) are commonly present in the basal ganglia and tend to increase in size and number with age. Since the cavities have different electrical and thermal properties compared with brain tissue, it is likely that they can affect the lesioning process and thereby the treatment outcome. Computer simulations using the Finite Element Method (FEM) and in-vitro experiments have been used to investigate the impact of cysts on lesions' size and shape. Simulations of the electric current and temperature distributions as well as convective movements have been conducted for various sizes, shapes and locations of the cysts as well as different target temperatures. Circulation of the CSF caused by the heating was found to spread heat effectively and the higher electric conductivity of the CSF increased heating of the cyst. These two effects were together able to greatly alter the resulting lesion size and shape when the cyst was in contact with the electrode tip. Similar results were obtained for the experiments.

## ***Short title***

Impact of cysts during RF-lesioning in deep brain structures

## 1. Introduction

Safe navigation towards the target and accurate determination of the effective target volume is of utmost importance in functional neurosurgery, e.g. radio frequency (RF) lesioning [1] or deep brain stimulation (DBS) [2]. During such stereotactic interventions the actual instrument or electrode is introduced to the target point and the operation is performed. Different nuclei in thalamus or in the basal ganglia belong to the commonly used mm-sized targets for deep brain surgery in order to reduce symptoms caused by e.g. chronic pain, psychiatric illness or movement disorders such as Parkinson's disease [3].

RF-lesioning (RF-ablation) is an electrosurgical method for e.g. neutralisation of malfunctioning signal pathways [3]. A high frequency alternating current gives rise to resistive heating followed by tissue coagulation in the vicinity of the electrode tip used for treatment. A temperature sensor, e.g. a thermocouple, in the electrode tip is used to control the current in order to maintain a preset target temperature and avoid, for instance, desiccation of the tissue. The method can also be used for treatment of, for example, cardiac arrhythmias [4] and cancer metastases [5].

The growth, size and shape of RF-lesions are influenced by many factors such as the electrical and thermal conductivities of tissue, electrode configuration and RF-generator settings including temperature, power and time. Our group has used the finite element method (FEM) for the simulation of RF-lesioning in several previous investigations. Studied topics are e.g. coagulation of an albumin rich test solution [6], impact of thermocouple location [7], the influence on lesion size from electrode design [8], blood perfusion, target temperature and the electrical and the thermal properties of brain matter [9]. In the latter study coagulation dependent thermal conductivity was introduced. Simulated data have been compared both with data from experimental test solution lesions [6] and in-vivo data from animal studies [9, 10].

Another issue of importance for the lesion development may be the perivascular Virchow-Robin (VR) spaces. Cysts, such as enlarged VR-spaces with cerebrospinal fluid (CSF), are common in the basal ganglia, also in young and healthy individuals [11]. VR-spaces surround the arterioles entering the brain and are believed to either be a part of the subarachnoid space or separate closed compartments [12]. These spaces are known to increase in size with age [11] as the brain slowly shrinks and lost tissue is replaced with CSF and its impact on DBS has been another topic of simulation studies by our group [13].

CSF has a considerably higher electric conductivity than brain tissue, which affects the current distribution along with the associated Joule heating and thereby the lesion size and shape. In combination with the ability of convective heat transfer such cavities can be suspected to have important impact on the size and shape of the created lesion. This has to our knowledge not been investigated in detail before. The aim of this study was to investigate and clarify the impact of CSF-filled cavities on resulting RF-lesion size and shape, and thus target volume. Both experimental and simulation models were used in order to investigate the potential effect of convective movements inside brain cysts.

## 2. Materials and Methods

A previous developed model using coagulation dependent thermal conductivity [9] was improved in order to also include effects of the heat transfer from convective movements in fluid-filled cavities. Experiments in kidney tissue and corresponding computer simulations were carried out in order to investigate whether the convection is important and if the simulations give reasonable results.

### 2.1.1 Governing Equations

The electric potential field,  $V$  (V), around the electrode was calculated using the equation of continuity for steady currents [14]:

$$\nabla \cdot \mathbf{J} = -\nabla \cdot [\sigma(T)\nabla V] = 0 \quad (\text{A/m}^3) \quad (1)$$

Here  $\mathbf{J}$  denotes current density ( $\text{A/m}^2$ ),  $T$  temperature ( $^\circ\text{C}$ ) and  $\sigma(T)$  temperature dependent electric conductivity ( $\text{S/m}$ ).

The temperature field,  $T$ , was calculated using the energy equation [15] with terms for convective heat flux,  $\rho c T \mathbf{u}$ , [16] and resistive heating [14]:

$$\rho c \frac{dT}{dt} = \nabla \cdot (k \nabla T - \rho c T \mathbf{u}) + \sigma(T) (\nabla V)^2 \quad (\text{W/m}^3) \quad (2)$$

Here  $\rho$  denotes mass density ( $\text{kg/m}^3$ ),  $c$  specific heat capacity ( $\text{J}/(\text{kg}\cdot\text{K})$ ),  $t$ , time (s),  $k$  thermal conductivity ( $\text{W}/(\text{m}\cdot\text{K})$ ) and  $\mathbf{u}$  velocity of the CSF or saline (m/s). The thermal effect of blood perfusion for living tissue was modelled as a locally increased thermal conductivity where a term due to blood perfusion,  $k_{\text{perf}}$ , is added to the thermal conductivity of the tissue itself  $k_{\text{tissue}}$

[17, 18]. This is considered the best standard model for flow dominated by microcirculatory vessels with a diameter of 200  $\mu\text{m}$  or less [17] and should thus be suitable for the central brain. Coagulation is assumed to inhibit blood perfusion in tissue heated to 60  $^{\circ}\text{C}$  [9]:

$$k = k(T) = \begin{cases} k_{tissue} + k_{perf} & (T \leq 60^{\circ}\text{C}) \\ k_{tissue} & (T > 60^{\circ}\text{C}) \end{cases} \quad (\text{W}/(\text{m}\cdot\text{K})) \quad (3)$$

The velocity field,  $\mathbf{u}$ , and static pressure field,  $p$  ( $\text{N}/\text{m}^2$ ), in the CSF and saline were calculated using Navier-Stokes equations for incompressible flow with gravitational (buoyancy) force [19], [20]:

$$\begin{cases} \rho \frac{\partial \mathbf{u}}{\partial t} + \rho(\mathbf{u} \cdot \nabla)\mathbf{u} = \nabla \cdot \{ \eta(T) [\nabla \mathbf{u} + (\nabla \mathbf{u})^T] \} - \nabla p + \rho(T)\mathbf{g} & (\text{N}/\text{m}^3) \\ \nabla \cdot \mathbf{u} = 0 & (\text{s}^{-1}) \end{cases} \quad (4)$$

Here  $\eta(T)$  denotes temperature dependent dynamic viscosity ( $\text{Pa}\cdot\text{s}$ ),  $\rho(T)$  temperature dependent mass density ( $\text{kg}/\text{m}^3$ ) and  $\mathbf{g}$  gravitational acceleration ( $\text{m}/\text{s}^2$ ).

### 2.1.2 Modelling and Simulation

Axi-symmetric models of a monopolar electrode with a tip length of 4 mm, electric insulation length of 2 mm and a diameter of 1 mm (for use with Leksell<sup>®</sup> Neuro Generator, Elekta Instrument AB, Sweden) surrounded by grey matter with and without CSF-filled cysts were set up (Figure 1a, Table 2). In addition, electrode models of the same geometry but surrounded with kidney tissue with and without a layer of saline were defined (Figure 1b, Table 3).

The electrode tip was set to hold a maximal voltage,  $V_{max}$ , of 25 V except for brain simulation 12 and kidney simulation 27 where 30 V was needed for sufficient power output and brain simulation 24 where 35 V was needed. The outer boundary was set to ground ( $V = 0$  V) on the lower part and to electric insulation (normal component of  $\mathbf{J} = 0$   $\text{A}/\text{m}^3$ ) on the upper part. If the upper part of the boundary were to be set to ground the upper part of the electrode would come into contact with ground. This would cause it to act as a bipolar electrode, which is not intended. The entire boundary had a prescribed constant temperature,  $T_0$ , of 37  $^{\circ}\text{C}$  for the brain models and 20  $^{\circ}\text{C}$  for the kidney models. The outer boundary was spherical with the radius 30 mm, which is sufficient for the solution to be independent of the boundary location. A point corresponding to the location of the thermocouple in the tip of the electrode was used to control the voltage of the tip in order to make the temperature of the thermocouple,  $T_{tip}$ ,

reach and hold a preset target temperature,  $T_{set}$ , and to limit its temperature increase to  $6\text{ }^{\circ}\text{C/s}$ . This control was implemented using logistic functions [21]:

$$V_{tip} = V_{max} \frac{1}{1 + \exp[5(T_{tip} - T_{set})]} \cdot \frac{1}{1 + \exp[5(T_{tip} - 6t - T_0)]} \quad (\text{V}) \quad (5)$$

The cavity with CSF in the simulations was assumed to have rigid walls with no slip ( $\mathbf{u} = 0$  m/s) and the CSF was assumed to be affected by the acceleration of gravity,  $g$ , of  $9.8\text{ m/s}^2$  [22] downwards, see Figure 1. The same conditions were applied to the saline in the kidney models except that frictionless tangential flow on the upper boundary was permitted. The initial conditions for the simulations were a temperature of  $37\text{ }^{\circ}\text{C}$  in the entire model and zero velocity in the CSF. The used material parameters can be seen in Table 1. For grey matter, blood perfusion was modelled as an increase in effective thermal conductivity  $k_{perf}$ , of  $0.5\text{ W/(K}\cdot\text{m)}$  in non-coagulated tissue. In cases of temperatures surpassing  $100\text{ }^{\circ}\text{C}$  the model is not valid. However, for comparison between simulations the material parameters were assumed to be the same as for  $100\text{ }^{\circ}\text{C}$  and the result was noted as an occurrence of boiling. The electric conductivity of the cavity fluid used in the simulations corresponds to the conductivity at  $10\text{ kHz}$ . This is not a problem as the electric conductivity of aqueous solutions is approximately constant for frequency between  $10\text{ kHz}$  and  $1000\text{ kHz}$  [23]. Water mass density,  $\rho$ , and dynamic viscosity,  $\eta$ , decrease non-linearly with temperature. While the density decrease is small, only  $4\%$  for the interesting interval of  $20\text{ }^{\circ}\text{C}$  to  $100\text{ }^{\circ}\text{C}$ , it is still sufficient to cause considerable convective movements in the CSF.

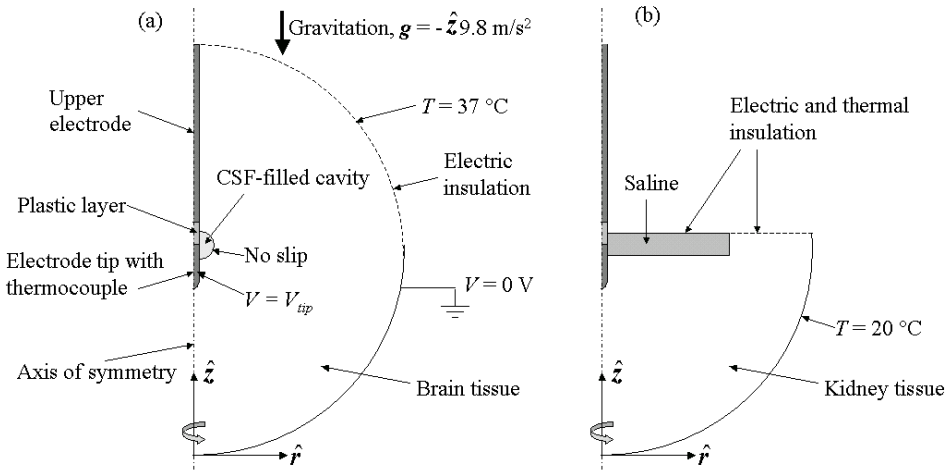


Figure 1: Model geometry and boundary conditions for axially symmetric brain (a) and kidney (b) models with gravitation downwards the  $\hat{z}$ -axis. The voltage of the electrode tip,

$V_{tip}$ , is controlled so that the temperature of the tip reaches and holds a preset temperature. The lower part of the outer boundary is assigned to ground ( $V = 0$  V). The no slip condition means zero convection ( $\mathbf{u} = 0$  m/s) at the boundaries of the CSF and saline. The upper part of the saline is in contact with air however permitting convection in the tangential direction.

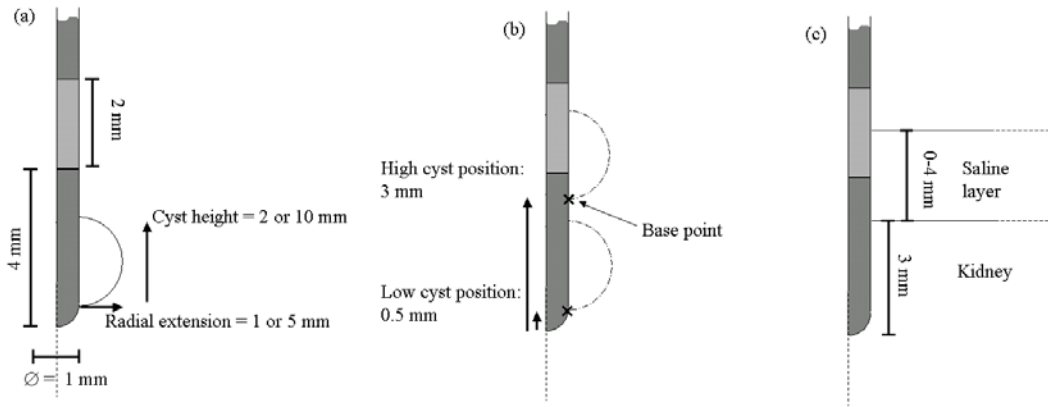


Figure 2: (a): Magnification of the electrode tip with variations of height and radial extension of the cyst resulting in four basic shapes: a small cyst, a thin cigar-shaped cyst, a flat disc-shaped cysts and a large cyst. (b): Position of the cyst. The base point  $\mathbf{x}$  of the cyst is measured in the  $\hat{z}$ -direction from the outermost tip of the electrode tip and is located beneath the electrode at  $-3$  mm, in a low position at  $0.5$  mm, in a high position at  $3$  mm or above the electrode tip at  $5$  mm. (c): Kidney models with no saline layer (simulation 25), a thin  $1$  mm saline layer (simulation 26) and with a  $4$  mm thick saline layer over the kidney surface (simulation 27).

The models were implemented in Comsol Multiphysics 3.2 (Comsol AB, Sweden). In total 24 simulations of the electrode in grey matter with and without CSF-filled cavities were made. Simulations numbered 1-20 included CSF-filled cavities with convective movements. The simulations were carried out for various target temperatures ( $70$  °C,  $80$  °C and  $90$  °C), base point position and sizes (height and radial extension) of the cavity (Table 2). The height was  $2$  mm or  $10$  mm, and the radial extension was  $1$  mm or  $5$  mm from the electrode surface (Figure 2a) giving four different basic shapes: a small cyst with a volume of  $9$  mm<sup>3</sup> ( $4$  mm<sup>3</sup> if beneath the electrode), a thin cigar-shaped cyst of  $46$  mm<sup>3</sup>, a flat disc-shaped cyst of  $129$  mm<sup>3</sup> and a large cyst of  $647$  mm<sup>3</sup>. Its base point position was at  $-3$  mm (cyst beneath electrode),  $0.5$  mm (low cyst position),  $3$  mm (high position) or  $5$  mm (cyst above electrode tip) upwards from the very tip of the electrode to the lowest point of the cyst (Figure 2b). Reference simulations without any CSF (No. 21-22), with CSF with no convective movements (No. 23) and with

CSF that was assumed to have as low electric conductivity as grey matter (No. 24) were also made in order to elucidate the importance of convection.

For the electrode simulations with kidney as surrounding tissue (No. 25-27) the target temperature was set to 80 °C and the electrode inserted 3 mm into the tissue (base point position at 3 mm). Simulations of lesion size with a saline layer (1 or 4 mm) covering the kidney were compared to the lesion extension without saline (Figure 2c, Table 3).

**Table 1.** Material properties. The saline is assumed to have the same properties as CSF.

	Electric conductivity, $\sigma$ (S/m)	Mass density, $\rho$ (kg/m <sup>3</sup> )	Specific heat capacity, $c$ (J/(kg·K))	Thermal conductivity, $k$ (W/(m·K))	Dynamic viscosity, $\eta$ (Pa·s)
Grey matter	$0.18 \cdot (1 + 0.018 \cdot (T - 20))$ <sup>a</sup>	$1.04 \cdot 10^3$ <sup>b</sup>	$3.68 \cdot 10^3$ <sup>b</sup>	$0.57$ <sup>b</sup>	(Not used)
Cerebrospinal fluid	$1.46 \cdot (1 + 0.02 \cdot (T - 22))$ <sup>c</sup>	$1.01 \cdot 10^3$ $1.01 \cdot \rho_{\text{water}}(T)$ <sup>d</sup>	$4.19 \cdot 10^3$ <sup>e</sup>	$0.60$ <sup>e</sup>	$1.02 \cdot \eta_{\text{water}}(T)$ <sup>f</sup>
Kidney	$0.2 \cdot (1 + 0.009 \cdot (T - 20))$ <sup>g</sup>	$1.05 \cdot 10^3$ <sup>b</sup>	$3.60 \cdot 10^3$ <sup>b</sup>	$0.55$ <sup>b</sup>	(Not used)
Electrode cover	$6.0 \cdot 10^6$ <sup>h</sup>	$4.75 \cdot 10^3$ <sup>a</sup>	$0.70 \cdot 10^3$ <sup>a</sup>	$9.0$ <sup>a</sup>	(Not used)
Plastic layer	(Not used)	$2.37 \cdot 10^3$ <sup>a</sup>	$1.30 \cdot 10^3$ <sup>a</sup>	$3.7$ <sup>a</sup>	(Not used)
Electrode tip	(Not used)	$6.0 \cdot 10^3$ <sup>a</sup>	$0.62 \cdot 10^3$ <sup>a</sup>	$11.5$ <sup>a</sup>	(Not used)

<sup>a</sup> Averaged values [24] (Based on [25], [26], [27] and [22])

<sup>b</sup> [26]

<sup>c</sup> At 10 kHz [28]

<sup>d</sup> [26] For purpose of gravity force, assumed to vary as water with temperature [29]

<sup>e</sup> Assumed to be identical to water [22]

<sup>f</sup> [26] Assumed to vary as water with temperature [29]

<sup>g</sup> Adjusted to 20 °C [30], [23] and [26]

<sup>h</sup> Stainless steel [22]

The simulated lesion was assumed to consist of all grey matter or kidney tissue reaching a temperature of 60 °C or more. The lesion's volume and widest diameter perpendicular to the electrode path was then determined. In addition, the maximal velocity,  $|u|$ , and maximal deviation from the target temperature at any point or time in the simulation and the initial ( $t = 0$  s) electric resistance between the electrode tip and ground was noted.

## 2.2 In-vitro Experiments

Experiments were carried out in order to verify the presence and importance of convective movements in the cyst in the vicinity of the active part of the electrode. It is not practically possible to experimentally investigate the convective movements for the normal geometry of Virchow-Robin spaces. Instead lesions were generated at the surface of pig brain obtained from a slaughterhouse (Blå kustens kontrollslakteri AB, Sweden). The experiments were performed with the brain at room temperature submerged in a saline solution (0.9 % NaCl) leaving a thin layer of solution above the lesioning site. The use of brain in the experiments was approved by the Swedish Board of Agriculture (D.no. 38-6097/05). Due to the difficulties with the brain's structure and geometry analogous lesions were generated in

kidneys, which have approximately the same electric and thermal properties as grey matter (Table 1). The kidneys were obtained from a grocery store.

Experiments in the brain were carried out for solution heights of about 1 and 3 mm and with the electrode tip inserted vertically 3 mm into the tissue leaving 1 mm in the saline. In order to make them easily visible the lesions were made in fissures and at a target temperature of 90 °C. For better-controlled experiments shallow holes with a flat surface were cut out in the kidneys. The electrode tip was also here inserted 3 mm into the tissue and three different experiments were performed; one with no saline solution covering the surface, one with 1 mm saline solution and one with 4 mm saline solution. Lesions were made at a target temperature of 80 °C for 60 s. After lesioning, the brain and kidney lesions were excised and cut through the middle of the electrode trajectory in a plane orthogonal to the surface. Photographs were then taken of this plane.

### 3. Results

Figures 3-6 exemplify the temperature distribution, lesion size and convective movements for some of the most interesting simulations after 60 s. The colour scales in the figures represent the temperatures and are capped at 100 °C. The 60 °C isotherm is also presented and it is marked with a thick white line in the grey matter and kidney tissue where it represents the calculated lesion contour. The velocity of the CSF or saline,  $\mathbf{u}$ , is represented by arrows that are roughly proportional in length to the absolute value of the velocity,  $|\mathbf{u}|$ . A summary of all brain simulations is presented in Table 2. Kidney simulations and experiments are summarised in Table 3.

The convection had a maximal absolute velocity of about 0 mm/s to 14 mm/s in the simulations with generally higher speeds for larger cysts. Convective movements in the cyst affect the lesions' sizes to a great extent, which is demonstrated in Figure 3. Simulation 22 (Figure 3a) is a reference simulation without a cyst and with a target temperature of 80 °C and simulation 23 (Figure 3b) is a reference simulation with a large cyst at low position but where the convection due to the heating is omitted. The difference between the simulations is solely dependent on the electrical properties of the cyst compared with brain tissue, and this alone is sufficient to increase the size of the lesion. The high electrical conductivity of the CSF in the cyst lowers the resistance between the tip and ground, especially when the cyst is in contact with the electrode tip as in models 1-17 and 23. The about 8 times higher electric conductivity of the CSF compared to the grey matter (Table 1) also focuses the current density to it since a

larger proportion of a current will go through the medium of lower resistance when parallel paths are available. As a consequence, the current density becomes high in the CSF at the upper part of the active tip for those simulations. This can be seen as a locally high temperature, more than 20 °C above the target temperature, beyond the model validity (> 100 °C) in simulation 23.

If only the convection is considered and the cyst otherwise is assumed to have the same electric conductivity as grey matter (simulation 24, Figure 3c) the convective heat transfer mitigates the heating over the cyst. Here a locally high temperature beyond the model validity appears in the grey matter beneath the electrode tip instead as the tip is cooled. When both the higher electric conductivity and the convective heat transport is included (simulation 12, Figure 3d) a larger lesion is obtained, but the maximum temperature is somewhat decreased compared with simulation 23. The maximum temperature in all simulations was obtained just outside the active electrode tip where the most intense Joule heating occurs, whereas the electrode is heated by heat conduction from the heated tissue. In pure grey matter the electrode tip corresponded well to the maximal temperature.

Figure 4 shows simulations of cysts with different sizes and locations. The higher electric conductivity of the CSF increases Joule heating of the cyst and the convective flow efficiently spreads heat extending the lesion for most simulations compared to reference simulation 22 without a cyst (Figure 3a). In simulation 16 (Figure 4h) however the large cyst at the high position makes the lesion smaller. A higher target temperature,  $T_{\text{set}}$ , increases the lesion size and convective velocity as can be seen in Figure 5. Further results are given in Table 2 where it can be seen that both larger and smaller lesions can be obtained when a cavity is present in the vicinity of the electrode tip.

**Table 2.** Parameters and results for the simulations.

Simulation number	Cyst height (mm)	Radial extension (mm)	Base point position (mm)	Target temperature (°C)	Deviation from target temperature (°C)	Max velocity $ u $ (mm/s)	Lesion volume (mm <sup>3</sup> )	Lesion diameter (mm)	Resistance at t = 0 s (Ω)
1	2	1	0.5	70	0.2	0.7	28.1	4.0	252
2	10	1	0.5	70	18.5	4.6	35.6	4.3	173
3	2	5	0.5	70	6.7	3.1	34.7	7.2	151
4	10	5	0.5	70	11.1	10.8	6.5	6.1	102
5	2	1	3	70	6.3	1.5	32.7	3.9	240
6	10	1	3	70	23.0	4.6	25.5	3.6	209
7	2	5	3	70	15.8	5.0	43.4	7.5	166
8	10	5	3	70	14.6	10.7	11.5	2.5	149
9	2	1	0.5	80	0.2	0.9	67.1	5.1	252
10	10	1	0.5	80	7.1	5.5	95.8	5.4	173
11	2	5	0.5	80	7.4	3.6	114.7	9.7	151
12 <sup>a</sup>	10	5	0.5	80	13.5	13.6	189.3	11.0	102
13	2	1	3	80	6.4	1.7	77.1	5.0	240
14	10	1	3	80	19.8	5.3	56.2	4.4	209
15	2	5	3	80	13.2	5.6	114.3	9.4	166
16	10	5	3	80	9.9	11.3	27.2	3.6	149
17	2	5	0.5	90	7.5	4.1	232.5	10.9	151
18	2	1	5 <sup>b</sup>	80	2.8	0.4	40.5	3.7	330
19	10	5	5 <sup>b</sup>	80	4.1	3.9	37.3	3.6	329
20	2	1	-3 <sup>b</sup>	80	2.2	0.1	39.3	3.7	344
21	-	-	-	70	0.6	-	18.0	2.7	354
22	-	-	-	80	0.5	-	40.0	3.7	354
23 <sup>c</sup>	10	5	0.5	80	(23.3) <sup>d</sup>	-	(5.1)	(3.8)	102
24 <sup>e</sup>	10	5	0.5	80	(23.1) <sup>d</sup>	(11.3)	(13.6)	(3.4)	332

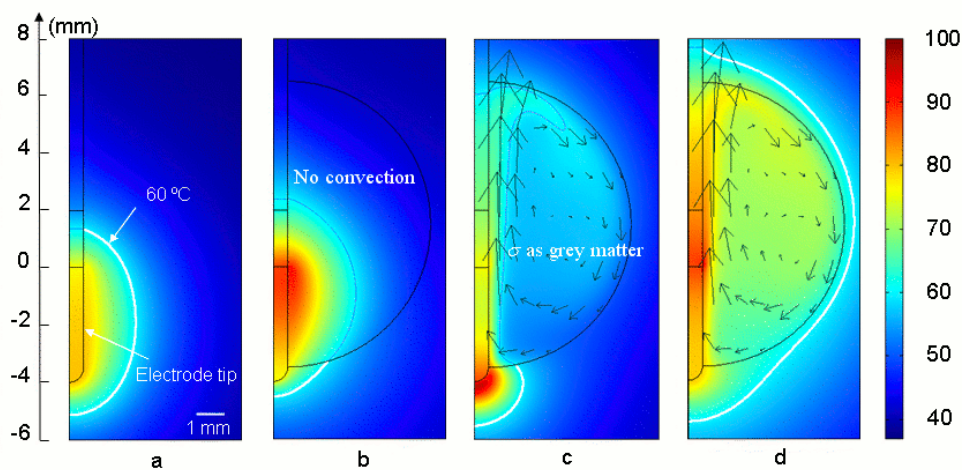
<sup>a</sup>  $V_{\max} = 30$  V<sup>b</sup> Cyst not in contact with electrode tip<sup>c</sup> No convective movements<sup>d</sup> Maximal temperature  $\geq 100$  °C<sup>e</sup> CSF assumed to have the same electric conductivity as grey matter,  $V_{\max} = 35$  V

Figure 3: (a) Simulated lesion without cyst (simulation 22), (b) with cyst but no convection (simulation 23), (c) with cyst and convection but with CSF assumed to have as low electrical conductivity as grey matter (simulation 24) and (d) with cyst with normal characteristics (simulation 12). The target temperature is 80 °C for all simulations. The 60 °C isotherm is included and marked white in the grey matter showing the lesion contour. The arrows show

the velocity field,  $\mathbf{u}$ , of the fluid. Comparing (a) and (b) it can be seen that the higher electric conductivity ( $\sigma$ ) of the CSF has concentrated the heating more to the cyst. If only considering the convection and assuming that the electric conductivity of the CSF is as low as that of grey matter (c) the convection mitigates the heat over a wide region. If both the higher electric conductivity of CSF and the convection is considered however the combination of increased heating of the cyst and enhanced thermal transport due to the convection creates a larger lesion (d).

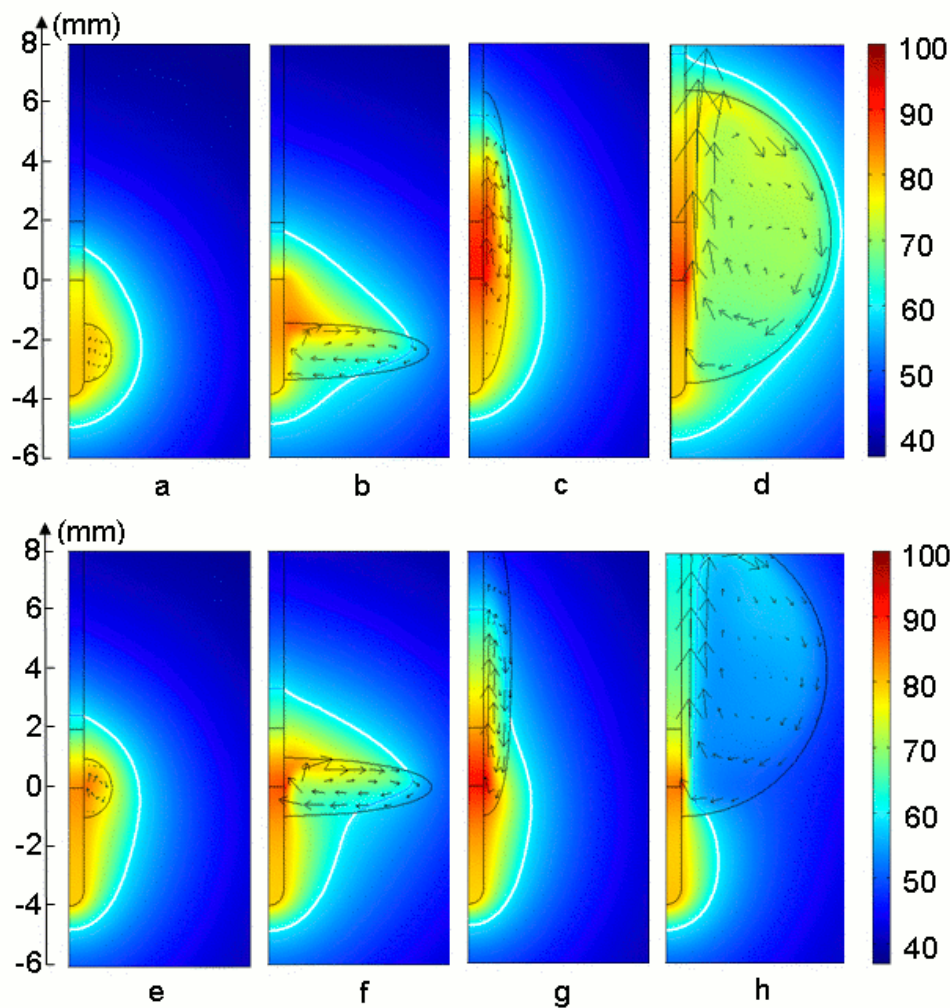


Figure 4: Simulations corresponding to models 9 to 16 in Table 2 (a-h respectively), all at a target temperature of 80 °C. Both the size and shape of the cyst have major impact of the size of the lesion extending it along the cyst for all simulations here except 16 (h). For the largest cysts (d and h) the location of the cyst is particularly important. A large lesion of 189 mm<sup>3</sup> is obtained in (d), but by relocating the cyst only 2.5 mm upwards a substantial decrease in lesion size is obtained (h). The lesion in (h) is even smaller than in Figure 3a (simulation 22)

where no cyst is present, which elucidates the possibility of the cyst to both heat and cool tissue in its vicinity.

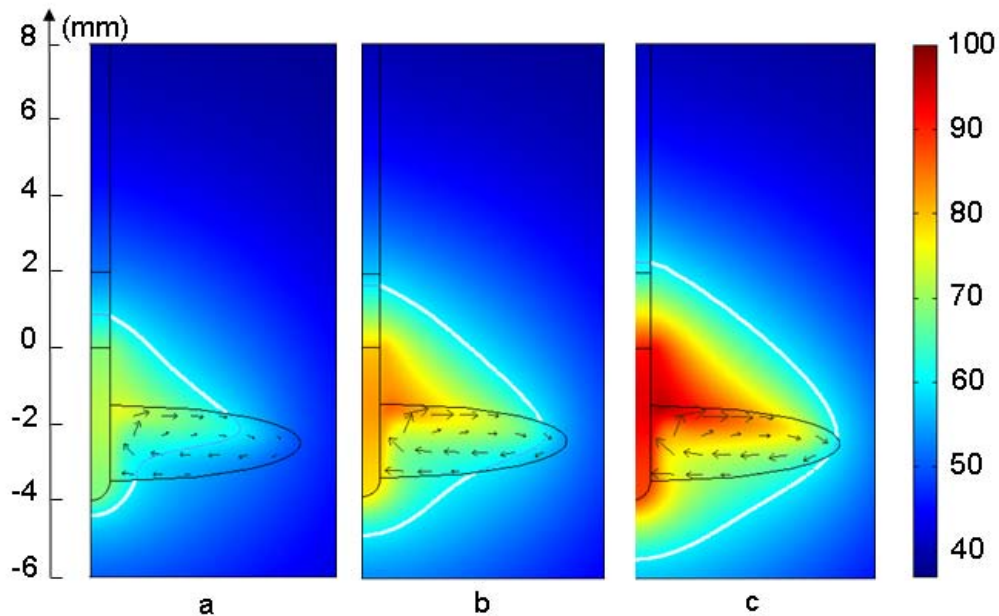


Figure 5: Simulations for one cyst geometry at three different target temperatures (70 °C, 80 °C and 90 °C) corresponding to simulations 3, 11 and 17, respectively. A higher target temperature results in a larger lesion.

The kidney simulations and corresponding in-vitro experiments (Figures 6 and 7) show that it is possible to substantially change the lesion size and shape by changing the electrical and thermal conditions of the lesioning process. The situation of no saline covering the kidney in simulation 25 (Figure 6a) results in an oval shaped lesion. Compared with this simulation 26 with a 1 mm high saline layer covering the surface (Figure 6b) shows a substantially larger lesion with a top-down pyramid shape, and simulation 27 with 4 mm saline covering the surface (Figure 6c) shows an oval lesion that is small, even smaller than in simulation 25. The simulated results agree well with the experiments shown in Figures 7a-c and Table 3. Similar results were obtained in brain tissue (Figure 8).

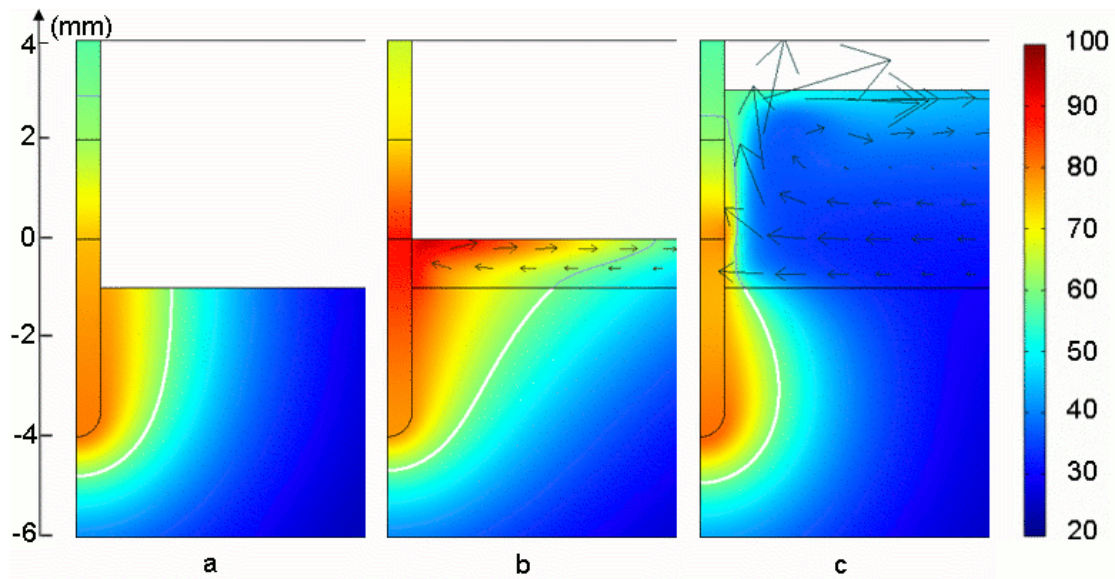


Figure 6: Simulations of the three kidney experiments. In (a) no saline is present. In (b) the higher electric conductivity of the saline concentrates more of the heating to the thin 1 mm saline layer and in (c) the high convective heat transfer of the thicker 4 mm saline layer negates this effect by cooling the surface of the lesion.

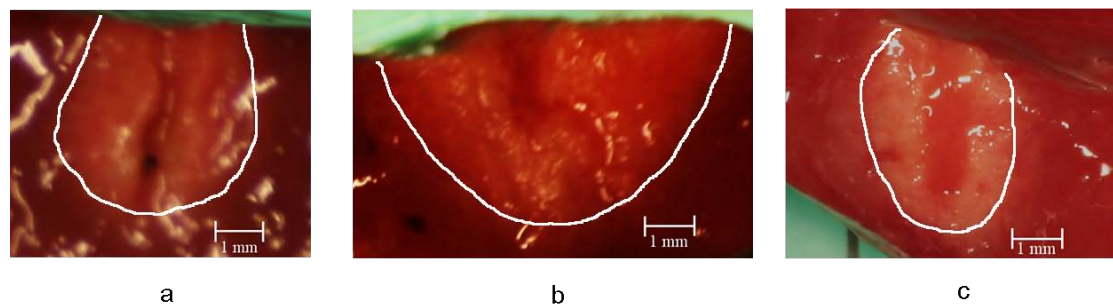


Figure 7: Experimental lesions in kidney in-vitro without saline solution (a) and with the kidney surface submerged in 1 mm and 4 mm of saline solution (b and c respectively) corresponding to the simulations presented in Figure 6 and visualized in the same plane orthogonal to the surface. The lesion contour is marked with white. As in the simulations (25 to 27, Figure 6) the thin 1 mm saline layer in (b) has extended the lesion along the surface while the higher convection in the thicker 4 mm layer (c) has cooled the surface making the lesion smaller.

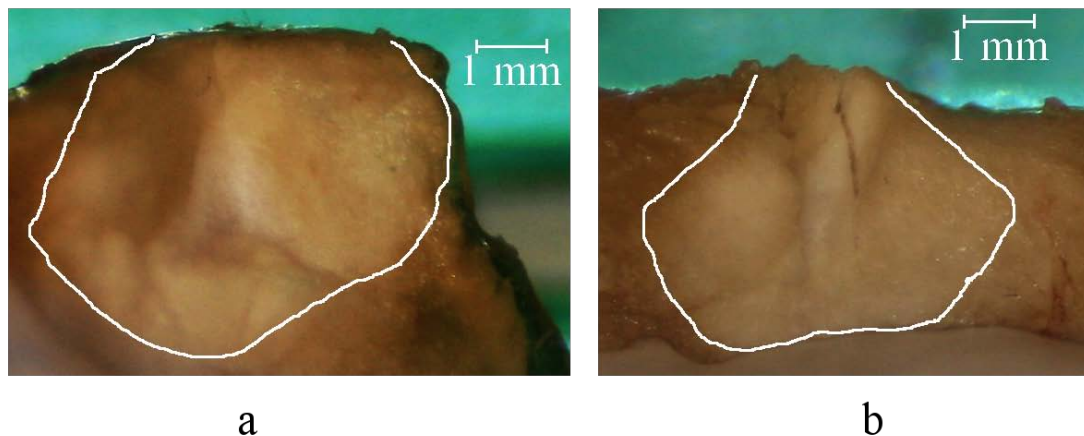


Figure 8: Experimental lesions in brain in-vitro with the brain surface submerged in 1 mm and 3 mm of saline solution (a and b respectively). While the surface is very rough the cooling of the larger amount of saline can still be seen in (b) as for the lesions in kidney tissue.

**Table 3.** Kidney simulations and experiments.

	Layer height (mm)	Base point position (mm)	Target temperature (°C)	Max velocity $ u $ (mm/s)	Deviation from target temperature (°C)	Lesion volume (mm <sup>3</sup> )	Lesion diameter (mm)
Simulation 25	0	3	80	-	1.2	30.5	3.9
Experiment 1	0	3	80	-	(unknown)	(unknown)	4.0
Simulation 26	1	3	80	2.9	16.4	50.0	6.7
Experiment 2	1	3	80	(unknown)	(unknown)	(unknown)	7.3
Simulation 27 <sup>a</sup>	4	3	80	10.0	2.1	20.5	3.2
Experiment 3	4	3	80	(unknown)	(unknown)	(unknown)	3.1

<sup>a</sup>  $V_{\max} = 30 \text{ V}$

#### 4. Discussion

In this study, both experiments and computer simulations were used to investigate the influence from natural convection in fluid-filled cavities known as Virchow-Robin spaces during radiofrequency (RF) thermal lesioning, and how the associated heat flux affects the therapy. The size, shape and location of Virchow-Robin spaces show considerable variability, and it is therefore impossible to cover all interesting possibilities in the analysis. The investigation was therefore focused on some interesting cases that together give relevant

information of the thermal effect, the importance of various parameters such as the cavity height and radius, and the distance from the electrode.

It can be concluded that the convective heat flux in the cyst can substantially change the size and shape of the lesion. The convective movements give rise to an increased heat flux, which can increase the lesion size. Enlargement is not guaranteed, however, since the heat may spread over a large volume. For example, in simulations 8 and 16 (Figure 4h) the large cyst at the high position has caused the lesion to become smaller instead. Studying Figure 4, it can be noted that the position of the cyst is of importance here. The influence of the small, the cigar-shaped and the disc-shaped cysts are similar for both the high and low position but the large cyst at the low position in model 12 (Figure 4d) has resulted in a larger lesion of 189 mm<sup>3</sup>. In earlier investigations by our group, based on experiments in-vitro in an albumin solution [31] and corresponding computer simulations [7], convective movements were found to substantially decrease the lesion size. Since the albumin solution used in those studies is a fluid itself, convection was possible in a relatively large volume surrounding the electrode. Here the convection actually increased the difference between target temperature and maximum temperature as opposed to this investigation and sometimes resulting in boiling of the solution. The difference may be due to the fact that much power was needed to compensate for convective losses and that coagulation of the albumin solution abruptly stopped the convection and corresponding convective heat transfer sometimes resulting in temperatures high enough to cause boiling locally near the tip. CSF does not coagulate and will continue to circulate.

Another important effect is that the relatively large electric conductivity of CSF in the cyst gives rise to a changed current distribution and thus a changed power deposition, temperature distribution and lesion size and shape [3]. Thus the entire treatment control is affected and the risk of CSF boiling is increased as can be seen by the temperatures above 100 °C obtained for a few cases even for a preset target temperature as low as 80 °C. Temperatures higher than 100 °C are possible in the simulations because vaporization is not included in the modelling. When the convective heat flux is included as in model 12 (Figure 3d), however, a much larger lesion but a lower maximum temperature is obtained. These effects taken together give interesting results for the kidney models with 1 and 4 mm saline layer respectively as well as for the corresponding experiments. When including a thin saline layer (simulation 26) the high electric conductivity of the saline causes high heating of the kidney surface and thus a relatively large lesion compared to a thicker saline layer (simulation 27), where large convective flow cooled the surface resulting in a smaller lesion. Similar results can be seen in

## Impact of cysts during RF-lesioning in deep brain structures

simulations 15 and 16. The disc-shaped cyst in simulation 15 (Figure 4f) has extended the lesion while the large cyst in simulation 16 (Figure 4h) has shrunk it.

A clinical aspect is that it might be possible to detect CSF-filled cavities prior to therapy. Since this tissue resistance can be measured prior to and during the lesioning process by the lesioning electrode itself, and since the cavities have a substantially different electric conductivity, the overall resistance may possibly be used as a complement to magnetic resonance imaging in order to detect potentially disruptive cysts before the lesioning procedure begins. The CSF in simulations 18 to 20, which is as close as 1 mm but not in contact with the tip, does not seem to have any considerable impact at all on lesion size. A clinical study by Laitinen et al. found no relation between the presence of cysts near the target spot and clinical outcome [11]. It is thus likely that the cysts only disturb the surgery when in the actual target area. However if in contact with the electrode tip the cysts might cause the creation of a larger lesion than intended as the temperature control compensates for the increased thermal transport by increasing the voltage in order to maintain the target temperature. This could result in undesirable side effects for the patient.

Symmetric geometries for the cysts were used together with an axi-symmetric overall geometry. This imposes some simplification of the flow field compared to a full 3D situation as secondary flow (see e.g. [32]) is ignored. The assumption of axial symmetry also requires the modelled electrode to be vertically oriented as the gravity force otherwise will not be axi-symmetric and also puts constriction on possible shapes and placements for the cysts. The assumption of incompressible flow may not be intuitive, as it is density variations that cause the convection here, but it is usually a sufficient approximation for liquids unless the pressure is extremely high. Other heterogeneities in the target area such as mixing of grey and white matter could be of interest to study. As thermal and electrical differences between grey and white matter are small compared to differences between grey or white matter and CSF, where the electric conductivity is about 8 times higher and convective heat transfer is possible, grey/white matter heterogeneities is expected to have minimal effect on tissue temperature distribution in comparison.

In conclusion it has been found that cysts in the vicinity of the therapeutic location can substantially affect the heating process and thereby the final size and shape of the generated lesion. The dominant factors are the convective movements with associated heat flux that occur in the CSF upon heating and the high electric conductivity of the CSF that increases its heating. Increasing convection can increase the lesion size to a certain extent but if the

## Impact of cysts during RF-lesioning in deep brain structures

convection becomes sufficiently large it may mitigate the heat over a wide region shrinking the lesion instead.

### **Acknowledgements**

We would like to thank the staff at Blå Kustens Kontrollslakteri AB, Florence Sjögren (Department of Biomedicine and Surgery, Linköping University), Ola Eriksson, Carina Fors and Mattias Åström (Department of Biomedical Engineering, Linköping University) for their valuable aid with the experiments. This work was supported by The Swedish Research Council for Engineering Sciences and Vinnova funded Competence Center Noninvasive Medical Measurements (Nimed).

## References

- [1] Hariz M I 2003 From functional neurosurgery to 'interventional' neurology: Survey of publications on thalamotomy, pallidotomy and deep brain stimulation for Parkinson's disease from 1966 to 2001 *Movement Disorder* **18** 845-53
- [2] Benabid A L, Koudsie A, Benazzouz A, Piallat B, Krack P, Limousin-Dowsey P, Lebas J F, and Pollak P 2001 Deep brain stimulation for Parkinson's disease *Adv Neurol* **86** 405-12
- [3] Cosman E 1996 Radiofrequency lesions *Textbook of Stereotactic and Functional Neurosurgery* ed Gildenberg P L and Tasker R (Kingsport: Quebecor Printing) pp 973-85
- [4] Tungjitkusolmun S, Woo E J, Cao H, Tsai J Z, Vorperian V R, and Webster J G 2000 Finite element analyses of uniform current density electrodes for radio-frequency cardiac ablation *IEEE Trans Biomed Eng* **47** 32-40
- [5] Goldberg S N 2001 Radiofrequency tumor ablation: principles and techniques *Eur J Ultrasound* **13** 129-47
- [6] Eriksson O, Wren J, Loyd D, and Wårdell K 1999 A comparison between in vitro studies of protein lesions generated by brain electrodes and finite element model simulations *Med Biol Eng Comput* **37** 737-41
- [7] Wren J, Eriksson O, Wårdell K, and Loyd D 2001 Analysis of temperature measurement for monitoring radio-frequency brain lesioning *Med Biol Eng Comput* **39** 255-62
- [8] Johansson J D, Wren J, Eriksson O, Loyd D, and Wårdell K 2005 Simulations of radio-frequency lesions with varying brain electrode dimensions *13th Nordic Baltic conference biomedical engineering and medical physics* (Umeå, Sweden) pp 62-3
- [9] Johansson J D, Eriksson O, Wren J, Loyd D, and Wårdell K 2006 Radio-frequency lesioning in brain tissue with coagulation-dependent thermal conductivity - modelling, simulation and analysis of parameter influence and interaction *Medical & Biological Engineering & Computing* **44** 757-66
- [10] Eriksson O, Backlund E-O, Lundberg P, Lindstam H, Lindström S, and Wårdell K 2002 Experimental radiofrequency brain lesions: a volumetric study *Neurosurgery* **51** 781-8
- [11] Laitinen L V, Chudy D, Tengvar M, Hariz M I, and Bergenheim A T 2000 Dilated perivascular spaces in the putamen and pallidum in patients with parkinson's disease scheduled for pallidotomy: A comparison between MRI findings and clinical symptoms and signs *Movement Disorder* **15** 1139-44
- [12] Edvinsson L and MacKenzie E T 2002 General and comparative anatomy of the cerebral circulation *Cerebral blood flow and metabolism* ed Edvinsson L and Krause D N 2 edit (Philadelphia: Lippincott Williams & Wilkins)
- [13] Åström M, Johansson J D, Hariz M I, Eriksson O, and Wårdell K 2006 The effect of cystic cavities on deep brain stimulation in the basal ganglia: a simulation-based study *Journal of Neural Engineering* **3** 132-8
- [14] Cheng D K 1989 *Field and wave electromagnetics* (USA: Addison-Wesley Publishing Company, Inc.)
- [15] Carslaw H S and Jaeger J C 1959 *Conduction of heat in solids* 2nd edit (Oxford: Oxford University Press)
- [16] Chen M M and Holmes K R 1980 Microvascular contributions in tissue heat transfer *Ann N Y Acad Sci* **335** 137-50

- [17] Wren J, Karlsson M, and Loyd D 2001 A hybrid equation for simulation of perfused tissue during thermal treatment *International Journal of Hyperthermia* **17** 483-98
- [18] Legendijk J, J.W. 1984 A new theory to calculate temperature distributions in tissues, or why the "Bioheat Transfer" equation does not work *Hyperthermic Oncology* ed Overgaard J (Basingstoke: Taylor and Francis) pp 507-10
- [19] Gresho P M and Sani R L 1998 *Incompressible flow and the finite element method* (Chichester: John Wiley & Sons Ltd)
- [20] Massoud M 2005 *Engineering thermofluids: thermodynamics, fluid mechanics and heat transfer* (Berlin: Springer Verlag)
- [21] Haykin S 1999 *Neural networks: a comprehensive foundation* 2 edit: Prentice-Hall, Inc.)
- [22] Nordling C and Österman J 1996 *Physics handbook for science and engineering* 5th edit: Studentlitteratur)
- [23] Gabriel S, Lau R W, and Gabriel C 1996 The dielectric properties of biological tissues: II. Measurements in the frequency range 10 Hz to 20 GHz *Physics in Medicine & Biology* **41** 2251-69
- [24] Johansson J D, Wren J, Loyd D, and Wårdell K 2004 Comparison between a detailed and a simplified finite element model of radio-frequency lesioning in the brain *26th Ann. Int. Conf. of the IEEE Eng. in Med. and Biol. Soc.* (San Fransisco, USA) pp 2510-3
- [25] Foster K R and Schwan H P 1989 Dielectric properties of tissues and biological materials: a critical review *Critical Reviews in Biomedical Engineering* **17** 25-103
- [26] Duck A F 1990 *Physical properties of tissue* (Cambridge: The University Press)
- [27] Holman J P 2001 *Heat transfer* 9th edit: McGraw-Hill Book company)
- [28] Baumann S B, Wozny D R, Kelly S K, and Meno F M 1997 The electric conductivity of human cerebrospinal fluid at body temperature *IEEE Transactions on Biomedical Engineering* **44** 220-3
- [29] Weast R C (ed) 1976 *Handbook of chemistry and physics* 57 ed: CRC Press
- [30] Andreuccetti D, Fossi R, and Petrucci C 1997-2002 *An Internet resource for the calculation of the Dielectric Properties of Body Tissues in the frequency range 10 Hz - 100 GHz* <http://niremf.ifac.cnr.it/tissprop/>
- [31] Eriksson O, Wårdell K, Bylund N E, Kullberg G, and Rehncrona S 1999 In vitro evaluation of brain lesioning electrodes (Leksell<sup>®</sup>) using a computer-assisted video system *Neurol Res* **21** 89-95
- [32] Schlichting H 1979 *Boundary-layer theory* 7 edit (New York: McGraw-Hill)